Electric Polarization Field of Phonon Modes Induced by Pressure and Maximally-Localized Wannier Functions in Beryllium Chalcogenides: Theoretical Study

ARTICLE *in* THE JOURNAL OF PHYSICAL CHEMISTRY C · JUNE 2011

Impact Factor: 4.77 · DOI: 10.1021/jp2017083

THE JOURNAL OF PHYSICAL CHEMISTRY C

ARTICLE

pubs.acs.org/JPCC

Electric Polarization Field of Phonon Modes Induced by Pressure and Maximally-Localized Wannier Functions in Beryllium Chalcogenides: Theoretical Study

S. Laref[†,‡,*] and A. Laref[‡]

[†]Université de Lyon, Institut de Chimie de Lyon, Laboratoire de Chimie, Ecole Normale Supérieure de Lyon, 46 Allée d'Italie, F−69364 Lyon Cedex 07, France

[‡]Physics Department, Science Faculty, University of Sidi Bel Abbes, Sidi Bel Abbes 22000, Algeria

Supporting Information

ABSTRACT: We present a theoretical study of polaron properties associated to the optical phonon modes induced by pressure on the beryllium chalcogenides. The calculations are performed using ab initio pseudopotential approach based on the density functional perturbation theory combined with maximally−localized Wannier functions. Features such as phonon frequencies, dielectric constants, effective polar field, polaron effective mass, Fröhlich coupling constant, Debye temperature, deformation potential, polaron diffusion constant, and maximally−localized Wannier functions have been determined. Good agreement is found between our simulated results and available data. In another case, our calculated values are totally predictive. We show that the pressure dependence of those physico−chemical considerations on the electric polarization field is found to vary monotonously. These studies form the basis for further development of models to describe polaron transport in the monocrystalline phase of BeX (X = S, Se, and Te) compounds such as bulk crystals.

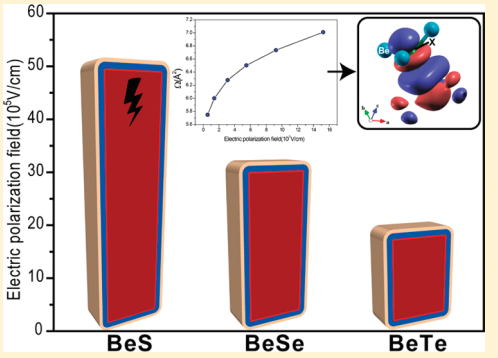

1. INTRODUCTION

The invention of new materials is critical for many potential innovative and clean energy technologies. The beryllium chalcogenides BeTe, BeSe, and BeS are II−VI compounds that crystallize at ambient pressure in the four-fold coordinated zinc-blend structure. Apart from BeO, which has a hexagonal structure, all of the other group-IIa chalcogenides adopt the rocksalt geometry. A unique feature in the beryllium compounds is that the Be ions are extremely small as compared to the anions except BeO.[1] This leads to an excess of the critical ratio of ionic radii, 4.45, for the zinc-blende structures in all three Be compounds; BeS, BeSe, and BeTe. Thus, unlike other IIa−VI compounds which are ionic, Be chalcogenides exhibit a high degree of covalent bonding with the Philips ionicities ranging from 0.169 in BeTe to 0.312 in BeS.[2] This class of semiconductors has indirect fundamental band gaps, which are associated with Γ−X transitions. Also, BeS has high hardness[3] while BeTe is a small gap semiconductor.[4] These interesting properties make them potentially useful for technological applications. Therefore, there is renewed interest in these compounds, which could be used in building green and blue light emitting electro-optical devices.[5] These compounds are of fundamental interest and possibly technological important due to their unusual or extreme properties.

Although extensive improvement has been made in theoretical explanation of the structural and electronic of II−VI beryllium chalcogenides compounds, many of their dynamical quantities are still not well-known. Understanding the effect of pressure on the phonon dispersion is the relative key for several fundamental and application studies of materials. Its knowledge allows one to correlate the results from an atomistic scale with macroscopic thermodynamic parameters. Experimentally, the phonon dispersion can be determined by many techniques such as electron energy loss spectroscopy, Raman spectroscopy, neutron scattering, IR absorption, and so forth. Moreover, the behavior of lattice vibrations under pressure provides useful information concerning bonding properties, phase transformations, structural instability, phonon−electron interactions, and carrier transport properties. It can be also used to study many thermodynamic phenomena, such as neutron diffraction spectra, Raman spectroscopy, thermal expansion, specific heats, and heat conduction.

To date, probably as a result of their very high toxic nature, which makes it difficult to obtain them as single crystals or epitaxial layers, only few experimental studies[5−7] have been performed on these compounds. Our results have been partially used to derive those works published 20 years ago for the photoemission spectrum of BeTe.[4] In order to comply with the renewed interest and to support the experiments with a theoretical database, we have performed a state-of-the-art first

Received: February 21, 2011
Revised: May 14, 2011
Published: May 23, 2011

dx.doi.org/10.1021/jp2017083 | J. Phys. Chem. C 2011, 115, 12604–12610

principles calculation of phonon modes of the three beryllium chalcogenides. Besides the inclusion of pressure and many-body energy shifts, we study in detail the dynamics of perturbed electrons manifested in their effective polar properties at a macroscopic level. These are completed using some basic equations.[8] In addition, we show that the behavior of the electric polarization field under pressure of these compounds is driven by the maximally−localized Wannier function.

The work is organized as follows. In Section II are present computational details. Section III gives the DFPT results for the lattice dynamics. In Section IV, the polaron properties under pressure with maximally−localized Wannier function are presented. Section V closes the work with conclusions.

2. METHODOLOGY

2. 1. Atomistic Calculations. The calculations were performed by means of the density functional theory implemented on Quantum ESPRESSO program package.[9] We used an ultrasoft Vanderbilt[10] formalism to the local density approximation (LDA).[11] The basis set for many-body interaction were described by a Ceperley and Alder functional parametrized by Perdew and Zunger.[12] The total-energy calculations were integrated over the Brillouin zone, by using a 4 × 4 × 4 Monkhorst−Pack method.[13] The pseudo-wave functions were expanded in a plane-wave basis set, with an energy cut-off of 55 Ryd treated in order to ensure convergence by an accuracy of 10^{-3} Ryd. The phonons vibrational modes were calculated from the optimized structure by employing density functional perturbation method (DFPT).[14] These quantities were calculated using a 4 × 4 × 4 Monkhorst−Pack scheme, which generate 10 k-points symmetrized in the irreducible Brillouin zone, this include the determination of the longitudinal optical/transverse modes (LO/TO) splitting at Γ point.

2. 2. Wannier Functions. Wannier functions provide a powerful tool to visualize and analyze bonding in extended systems.[15] A general transformation between the Bloch and Wannier representations is given by the following:

$$w_n(\mathbf{R}) = \int_{\mathrm{BZ}} \sum_m U_{mn}^{(\mathrm{k})} e^{-i\mathbf{k}\cdot\mathbf{R}} \psi_{m\mathbf{k}}(\mathbf{r}) d\mathbf{k} \quad (1)$$

where $U_{mn}^{(\mathrm{k})}$ is a unitary matrix. By defining a measure of the spatial spread functional of the Wannier functions

$$\Omega = \sum_n [\langle w_n(\mathbf{0})|r^2|w_n(\mathbf{0})\rangle - \langle w_n(\mathbf{0})|\mathbf{r}|w_n(\mathbf{0})\rangle^2] \quad (2)$$

In this work, the MLWFs are determined using the WANNIER90 code,[16] which only requires the overlap matrices and an initial guess of the projection of the Bloch states onto trial localized orbitals. Through a minimization procedure, a transformation matrix is computed which can be used to express the Hamiltonian of the system in the basis of the MLWFs.

2. 3. Macroscopic Calculations. The dielectric constant is a powerful quantity to clarify various phenomena in micro-electronics, optics-electronics, and solid-state physics. The dielectric constant is the relative permittivity of a dielectric material. It is an important parameter in characterizing capacitors. The knowledge of the dielectric constant of a material is needed to properly design and apply instruments such as level controls using radar, rf admittance, or capacitance technologies. In the present work, the high frequency dielectric constant ε_∞ has been derived from the DFPT calculation, whereas the static dielectric constant ε_0 was calculated using the Lyddane−Sachs−Teller formalism,[17]

Table 1. Calculated Static ε_0 and Macroscopic Dielectric Constant ε_∞, Born Effective Charge Z*, and Zone-Center Phonon Frequencies ω_{TO} and ω_{LO} in Unit of cm^{-1}[a]

	BeS	BeSe	BeTe
ε_0	7.29[b]	7.47[b]	8.59[b]
ε_∞	5.45[b]−5.46[d]	6.16[b]−6.1[c]−6.09[d]	7.66[b]−6.9[c]−7.51[d]
Z^*	1.53[b]−1.61[e]	1.47[b]−1.56[e]	1.24[b]−1.51[e]
ω_{TO}	566[b]−566[d]	501[b]−496[c]	476[b]−461[c]
ω_{LO}	655[b]−647[d]	561[b]−576[c]	505[b]−502[c]

[a] The results are compared with available theoretical and experimental results for BeS, BeSe, and BeTe. [b] Present work. [c] From ref 3. [d] From ref 28. [e] From ref 43.

$$\frac{\omega_{\mathrm{TO}}^2}{\omega_{\mathrm{LO}}^2} = \frac{\varepsilon_\infty}{\varepsilon_0} \quad (3)$$

where ω_{TO} and ω_{LO} represent the transverse and longitudinal phonon modes at the optical zone center.

The prototype of polaron is defined by electron conduction in optical polar semiconductor. The strength of the electron−phonon interaction is expressed by dimensionless coupling constant α_{F} introduced by Fröhlich,[16] this parameter is specified by the following expression:[18,19]

$$\alpha_{\mathrm{F}} = \frac{1}{2} \frac{e^2/(\hbar/2m^*\omega_{\mathrm{LO}})^{1/2}}{\hbar\omega_{\mathrm{LO}}} \left(\frac{1}{\varepsilon_\infty} - \frac{1}{\varepsilon_0}\right) \quad (4)$$

where m^* is the electron effective mass. In the present work, m^* is calculated in the conduction electronic band minimum at the Γ valley from the band curvature using the term,

$$\frac{1}{m^*} = \frac{1}{\hbar^2} \frac{d^2E(k)}{dk^2} \quad (5)$$

where E is the electron energy and k the wave vector in a periodic potential field of a semiconductor. In polar semiconductors, LO modes have an associated electric polarization field. The strength of this field can be expressed as follows:

$$E_0 = \frac{m^* e\omega_{\mathrm{LO}}}{\hbar} \left(\frac{1}{\varepsilon_\infty} - \frac{1}{\varepsilon_0}\right) \quad (6)$$

Another important physical quantity will be calculated as well Debye temperature θ_{PO} related to LO phonon frequency. These measured data are defined as follows:

$$\theta_{\mathrm{PO}} = \frac{\hbar\omega_{\mathrm{LO}}}{k_{\mathrm{B}}} \quad (7)$$

Formation and migration of polarons in bulk beryllium monochalcogenides were modeled using density functional theory (DFT) combined with the Kornilovitch model of Fröhlich polaron transfer[20]

$$\frac{1}{m^*} = \frac{2D}{\hbar} \quad (8)$$

where m^* is replaced by the electron effective mass of polaron, and D_{pol} is polaron diffusion coefficient.

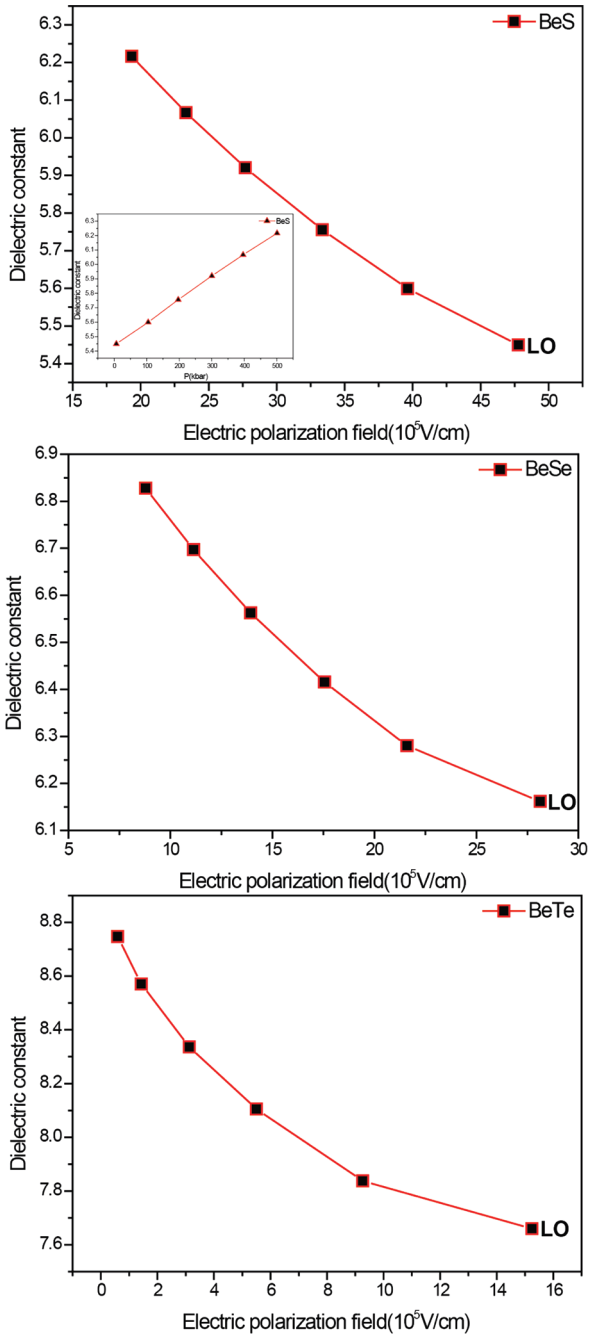

Figure 1. Macroscopic dielectric constant ε_∞ versus electric polarization field coupled with LO mode of BeX (X = S, Se, Te) compounds induced by pressure.

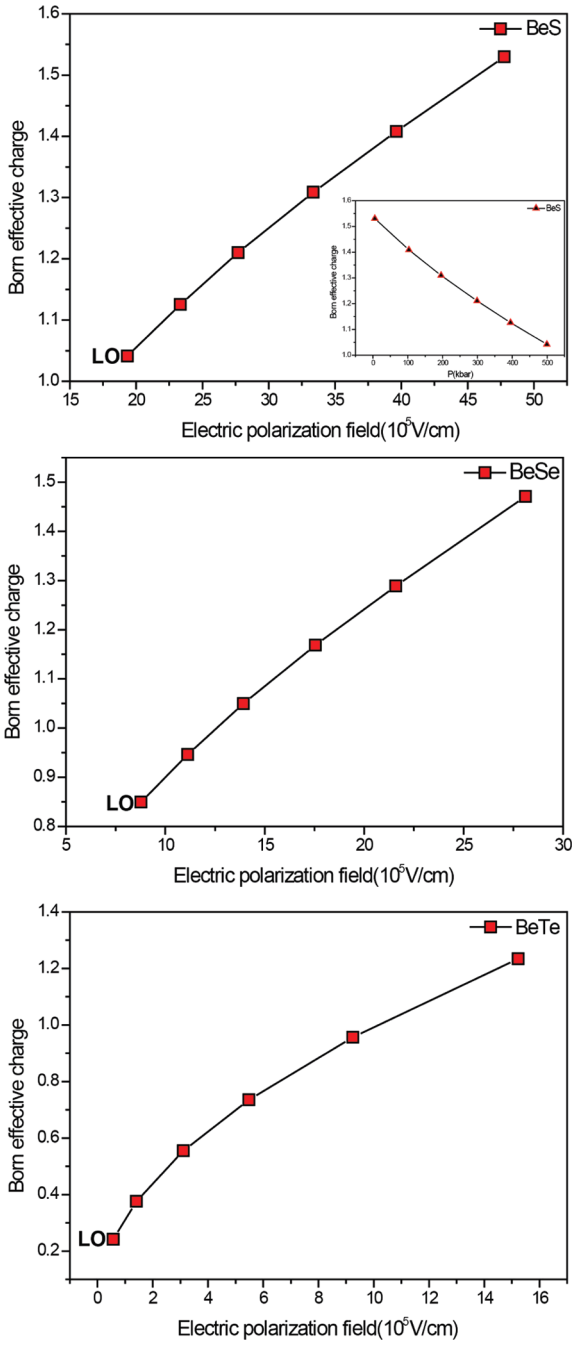

Figure 2. Born effective charge Z^* versus electric polarization field coupled with LO mode of BeX (X = S, Se, Te) compounds induced by pressure.

3. NUMERICAL RESULTS AND DISCUSSIONS

There are several data available regarding the polaron formation in a variety of materials.[21−25] Accurate polaron models at the atomic level may help address the issue of the stability of the polarons under hydrostatic pressure in different phases. The electron effect into the conduction band in perfect ionic crystals have an energy support, this is for it moving in the spatial localized state, accompanied by a local deformation in the previously perfect ionic arrangement (i.e., a polarization of the lattice) which serve to screen its field and reduce its electrostatic energy.[19] A conduction electron in an ionic crystal and/or a polar semiconductor is the prototype of a polaron. Conversely to the non−polar IV−IV semiconductors, the atomic displacements in polar materials create dipoles. The long-range macroscopic electric field accompanying several atomic relaxations in polar crystals is determined by a non-analytic contribution to the dynamical matrix,[26,27] consisting of the tensors of the Born effective charges $Z^{B(k)}$ and of the highest dielectric constants ε_∞.

In the zinc-blend structure, the tensors of the (transverse) Born effective charge and the high−frequency dielectric constants are isotropic. Because of the neutrality in the system, the charges of the cation and anion can differ only by the sign in some

dx.doi.org/10.1021/jp2017083 |J. Phys. Chem. C 2011, 115, 12604–12610

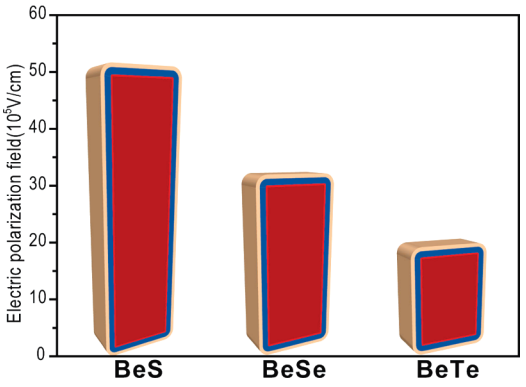

Figure 3. Electric polarization field coupled with LO mode of BeX (X = S, Se, Te) compounds at ambient pressure.

cases. Table 1 lists the calculated values for the dielectric tensor and the Born effective charge Z^* of BeS, BeSe and BeTe in the zinc−blende structures at zero pressure. For Z^* of BeS there is no experimental measurement while the theoretical data are available, and hence our results are in agreement with previous calculations.[43] However, for ε_∞, the only available value in the literature is that of 5.46 reported very recently by Srivastava et al.[28] as shown in Table 1. This value is in very good agreement with those obtained in the present calculation. However, in the case of BeSe and BeTe, we note that our results are in good agreement with those reported in refs 3, 4, and (see Table 1).

The variation of Z^* and ε_∞ as a function of pressure for BeS, BeSe, and BeTe in the zinc-blend structures are displayed in Figures 1 and 2. We see that as pressure P increases, Z^* decreases, while ε_∞ increases. Both behaviors are monotonous. Commonly, the polar semiconductors have an associated electric polarization field E_0 as expressed in eq 6. This E_0 is coupled with an LO mode and so−called effective polar field. It is important to know the electron mobility and electric field characterizations for high− devices in polar crystals. The predicted calculations of E_0 for BeS, BeSe, and BeTe compounds are illustrated in the Table 2. We note from these results that E_0 increase as well from BeS, BeSe, to BeTe. By implication, the hydrostatic pressure on E_0, we see a monotonous decrease for the three crystalline beryllium chalcogenides (Supporting Information, SI). This may conclude that the changing of dielectric constant reflects those variations in effective polar field by means of the polarization in the dielectric parameter.

Hence, the calculated electric polarization field from eq 6 is twice important in BeS than BeTe (see Figure 3). One may think also to the reduction of the electric field polarization associated to LO mode under compression since the Born charges also include a component due to a dynamic polarizability.[29] The pressure-induced reduction of the dynamical ion charges indicates a charge redistribution from the S, Se, and Te atoms to the Be atoms in comparison with the pressure-free situation. However, the increase of the dielectric constant with effective polaron field when pressure is raised implies that the dielectric capacity of the material of interest becomes better and hence the material becomes a good insulator.

We present in Table 2 the Fröhlich coupling constant introduced from electron effective mass obtained from eq 4. We observe that α_F decrease monotonically under hydrostatic pressure (Figure S2 of the SI) through a pseudo-linear shape in the case of BeS and BeSe, except for BeTe with plateau like in the

Table 2. Calculated Polarization Field E_0, Fröhlich Coupling Parameter α_F, Debye Temperature of the LO Phonon Frequency θ_{LO}, Deformation Energy Related to LO Mode, Polaron Effective Mass m^*_{pol}/m^*, and Polaron Diffusion Coefficient in BeS, BeSe, and BeTe Materials at Ambient Pressure

materials	E_0 (10^5 V/cm)	α_F	θ_{LO} (K)	E_D (eV)	m^*_{pol}/m^*	D_{pol} (10^{-13} cm^2/s)
BeS	47.79	5.11	980	0.211	4.13	2.68
BeSe	28.13	3.86	820	0.136	2.43	4.75
BeTe	15.24	2.10	737.5	0.067	1.5	5.44

front of the highest pressures. This might be due to the asymmetrical local deformation of the lattice, which becomes stronger from BeS (BeSe) to BeTe, respectively. We know from Adachi et al.[8] that α_F is strongly dependent on the ionic polarization of the crystal. They propose a suggestion considering that the mounting of α_F vary gradually with increasing the crystal ionicity. This general trend is not consistent with our results since according to the Phillip's ionicity scale[8,19,30] the ionicity factor (f_i) of BeS and BeSe (f_i = 0.29 and 0.26) is larger than BeTe (f_i = 0.17) compound. The pressure dependence of θ_{PO} is depicted in Figure S3 of the SI. We observe that θ_{PO} is enhanced with increasing the P parameters. This linear enhancement is monotonous. Generally, the highest Debye temperature reflects low atomic mass and thus short interatomic bond-length in A^NB^{8-N} semiconductors.[19] This is consistent with our calculated results (see Table 2).

The deformation energy E_D has also been calculated using the expression in the eq 9 below,

$$\frac{1}{2}\alpha_F = \frac{E_D}{\hbar\omega_{LO}} \tag{9}$$

We consider $\alpha_F/2$ as "the number of phonons which surround an electron that moves slowly inside a crystal." Our results regarding E_D for BeS, BeSe, and BeTe are given in Table 2. E_D of polaron increases monotonically exhibiting a deformation energy among 0.211, 0.136, and 0.07 eV, respectively, to BeS, BeSe, and BeTe, compounds. This weak values suggest an almost linear decreased when apply pressure. The increase of E_D leads to the increased in the quantity of $\alpha_F/2$ indicating thus that the number of phonons surrounding the electron moves slowly inside BeS and BeSe are more important than the number of phonons inside BeTe.

The electron-LO-phonon coupling is known to modify the electron effective mass.[8] It is noted that the mass measured in cyclotron resonance experiments in polar semiconductors is the polaron mass rather than the "bare" band-edge mass given by theoretical calculations of the band parameters.[8] The physical properties of a polaron differ from those of a band-carrier. A polaron is characterized by its self-energy, an effective mass m^*_{pol} and by its characteristic response to external electric and magnetic fields. The m^*_{pol} can be computed by means of Langreth formula as reported in refs 19 and 31.

$$m^*_{pol} = m^*\left(\frac{1 - 0.0008\alpha_F^2}{1 - \frac{\alpha_F}{6} + 0.0034\alpha_F^2}\right) \tag{10}$$

dx.doi.org/10.1021/jp2017083 |J. Phys. Chem. C 2011, 115, 12604–12610

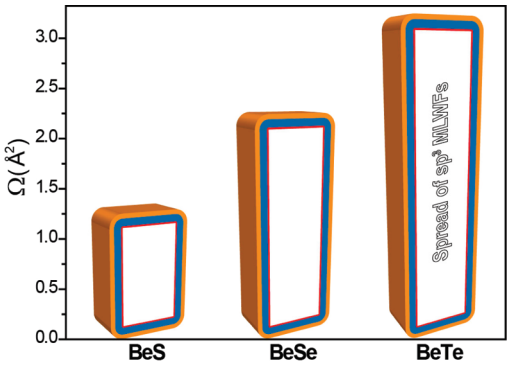

Figure 4. Spread of the sp^3 maximally-localized Wannier functions of BeX (X = S, Se, Te) at ambient pressure.

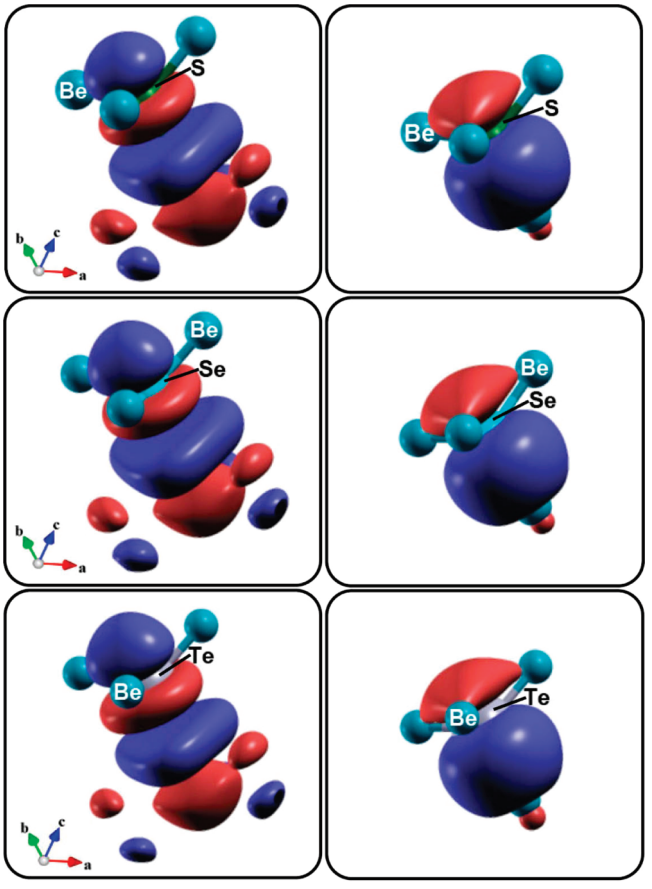

Figure 5. Maximally−localized Wannier functions of BeX (X = S, Se, Te) compounds at ambient pressure. The lowest unoccupied MLWFs are shown on the left and the highest occupied MLWFs on the right.

The variation in m^*_{pol}, shows that the mobility of the polarons changes by changing the anionic elements VI of the interest material (see Table 2), which may provide more diverse opportunities to describe most carrier transport properties on these materials and its alloys classes.

We previously modeled the formation of phonon−polaron in defect-free bulk zinc blend beryllium chalcogenides. In this section, we would like to include the transfer of the polarons along [111] direction. With regard to the calculated coefficient diffusion D_{pol} from smallest to highest anionic elements, we see

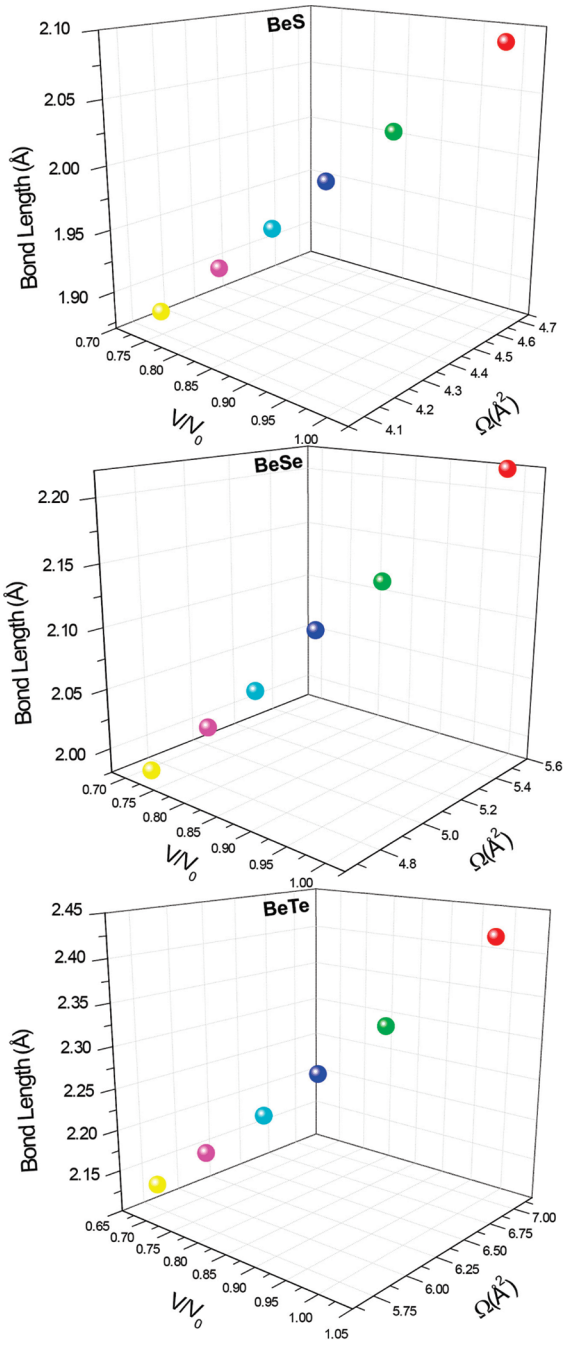

Figure 6. Total spread of occupied the MLWFs and Be−X (X = S, Se, Te) bond lengths as a function of volume.

that there is a fast diffusion in the [111] direction on such BeX (X = S, Se and Te) compounds. D_{pol} is two times more important in the case of BeTe (5.44×10^{-13} cm^2/s) than BeS (2.68×10^{-13} cm^2/s) and less significant than the BeSe (4.75×10^{-13} cm^2/s) semiconductor; this might be related to the moves by hopping or by propagation in a band ($E_g^{BeS} > E_g^{BeTe}$), and whether the scattering from impurities or phonon is dominant. In general, the diffusion constant is due to the longitudinal optic phonon scattering. For instance, comparing our results to the macroscopic diffusion coefficients in anatase films,[32−39] which vary from 10^{-10} to 10^{-17} cm^2/s. These last results are in agreement with our calculations (the same results in the range

dx.doi.org/10.1021/jp2017083 |J. Phys. Chem. C 2011, 115, 12604–12610

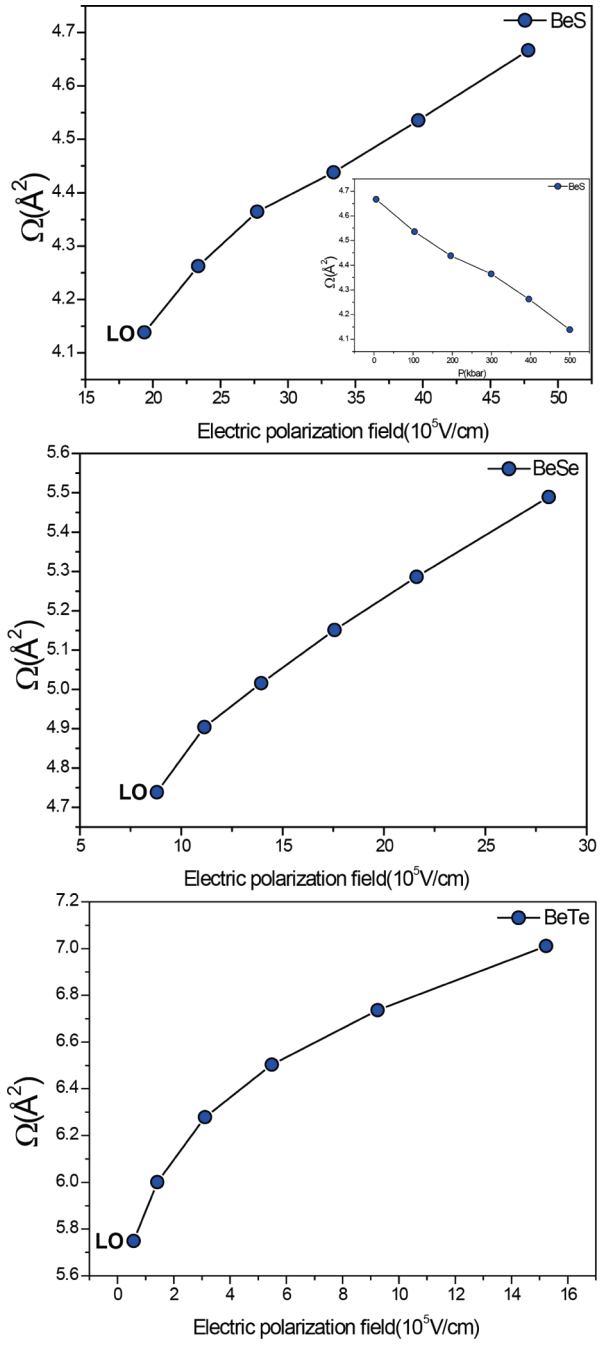

Figure 7. Total spread of occupied MLWFs versus electric polarization field coupled with LO mode of BeX (X = S, Se, Te) compounds induced by pressure.

illustrated above). Furthermore, Kavan et al.[37] has shown that the diffusion coefficient is close to $\sim 10^{-13}$ cm^2/s in anatase single crystals. Other experimental work[40] showed that the diffusion of electrons is faster than the diffusion of holes in nanocrystalline TiO_2.

Additionally, to further elucidate the nature of the electronic structure, we have performed an analysis of the maximally-localized Wannier functions as function of hydrostatic pressure versus effective polarization field. Before discussing the pressure effect to the spread of the MLWFs with regard to Figures 4 and 5, these IIa−VI compounds, have two atoms at the ends and each bond have different electronegativities. This leads to a partial charge transfer from the cation (Be) to the anion (S, Se, and Te) regions. This, in turn, shifts the center of the MLWFs away from the center of the bond toward the anion, as illustrated in Figure 5. It is interesting to note that, with respect to the anions, the MLWFs in the RS phase have the same orientation as those in the ZB phase (along the bonds of the latter structure).[41] Moreover, it is meaningful to consider that each MLWFs is a superposition of three somehow "optimized" σ-bond orbitals of the three neighboring bonds (see Figure 5). Thus, each bond yields two-thirds of the MLWFs, which is the same ratio between the number of MLWFs and the bonds in the ZB structure.[41]

In Figure 4, we show the sp^3 spread of MLWFs with respect to BeS, BeSe, and BeTe compounds. The spread is significant in BeTe (Ω_{min} = 7.01 Å^2) than BeSe (Ω_{min} = 5.49 Å^2) and BeS (Ω_{min} = 4.67 Å^2), respectively. The atomic size of beryllium is extremely small regarding to the atomic size of the chalcogenides elements, which make these classes of materials exceptional. For all compounds, the total spread with chemical bond length rises from its initial value at elevated pressures until the system reaches monotonous (see Figure 6). In the high pressure, no separation of occupied and unoccupied states can be made. We can, however, construct approximate MLWFs by considering all Bloch states up to the Fermi−level as fully occupied. This is justified since in this region, there is considerably less volume in the *k*-space around **R** where valence and conduction bands overlap.

Moreover, the total spread increases monotonically, accompanying the effective polar field by deducing the pressure in these Be−chalcogenide materials studies. The spread obtained in this trend rises roughly to a cusp. At sufficiently large volume, the system becomes insulating again and the spread continues to decrease involvement by high pressure (see Figure 7). Therefore, the MLWF spread reproduces the behavior expected for a system undergoing an insulator-metal-insulator transition.[42]

4. CONCLUSIONS

We have unveiled the nature of polaron properties related to the optical phonon modes deduced by hydrostatic pressure on beryllium chalcogenides, from an atomistic approach toward a macroscopic eye. We show that, using ab initio pseudopotential approach based on DFPT combined with maximally-localized Wannier functions. Characteristics, as well as phonon frequencies, dielectric constants, and spread center Wannier localized functions, have been determined. Good agreement is found between our calculated results and available data. In another case, our simulated value has been shown for the first time by means of an effective polar field, polaron effective mass, Fröhlich coupling constant, Debye temperature, deformation potential, and polaron transport in BeX (X = S, Se and Te) compounds. These results are for reference in these technologically interesting materials. The pressure dependence on the physicochemical kindness of the effective polar field has a monotonous variation. Moreover, the systematic analyses allow us to quantify the borders of the electric polarization field on beryllium monochalcogenides, which are coupled with optical zone center modes deduced by the hydrostatic pressure. Finally, this explicit work opens promising perspectives for the technological application of LED components.

■ ASSOCIATED CONTENT

Supporting Information. This material is available free of charge via the Internet at http://pubs.acs.org.

■ AUTHOR INFORMATION

Corresponding Author
* E-mail: laref_s@yahoo.fr.

■ REFERENCES

(1) Luo, H.; Ghandehari, K.; Greene, R. G.; Ruoff, A. L.; Trailand, S. S.; DiSalvo, F. *J. Phys. Rev. B* **1995**, *52*, 7058.
(2) Vechten, J. A. *Phys. Rev.* **1969**, *187*, 1007.
(3) Talwar, D. N. *Phys. Rev. B* **2010**, *82*, 085207.
(4) Nagelstrasser, M.; Dröge, H.; Steinrück, H.-P.; Fischer, F.; Litz, T.; Waag, A.; Landwehr, G.; Fleszar, A.; Hanke, W. *Phys. Rev. B* **1998**, *58*, 10394.
(5) Yim, W. M.; Dismakes, J. B.; Stofko, E. J.; Paff, R.-J. *J. Phys. Chem. Solids* **1972**, *33*, 501.
(6) Staritzky, E. *Anal. Chem.* **1956**, *28*, 915.
(7) Zachariasen, W. *Z. Physik Chem. (Leipzig)* **1926**, *119*, 210. **1926**, *124*, 440.
(8) Adachi, S. *Properties of Group IV, III−V and II−VI Semiconductors*; Wiley: Chichester, 2005.
(9) Baroni, S.; Dal Corso, A.; de Gironcoli, S.; Giannozzi, P. http://www.quantum-espresso.org. and Giannozzi, P.; Baroni, S.; Bonini, N.; Calandra, M.; Car, R.; Cavazzoni, C.; Ceresoli, D.; Chiarotti., G. L.; Cococcioni, M.; Dabo, I.; Dal Corso, A.; de Gironcoli, S.; Fabris, S.; Fratesi, G.; Gebauer, R.; Gerstmann, U.; Gougoussis, C.; Kokalj, A.; Lazzeri, M.; Martin−Samos, L.; Marzari, N.; Mauri, F.; Mazzarello, R.; Paolini, S.; Pasquarello, A.; Paulatto, L.; Sbraccia, C.; Scandolo, S.; Sclauzero, G.; Seitsonen, A. P.; Smogunov, A.; Umari, P.; Wentzcovitch, R. M. *J. Phys.: Condens. Matter* **2009**, *21*, 395502.
(10) Vanderbilt, D. *Phys. Rev. B* **1985**, *32*, 8412.
(11) Ceperley, D. M.; Alder, B. J. *Phys. Rev. Lett.* **1980**, *45*, 566.
(12) Perdew, J. P.; Zunger, A. *Phys. Rev. B* **1981**, *23*, 5048.
(13) Monkhorst, H. J.; Park, J. D. *Phys. Rev. B* **1976**, *13*, 5188.
(14) Baroni, S.; de Gironcoli, S.; Dal Corso, A.; Giannozzi, P. *Rev. Mod. Phys.* **2001**, *73*, 515.
(15) Silvestrelli, P. L.; Marzari, N.; Vanderbilt, D.; Parrinello, M. *Solid State Commun.* **1998**, *107*, 7.
(16) Marzari, N.; Vanderbilt, D. http://www.wannier90.org.
(17) Kittel, C. *Introduction to Solid−State Physics*, 5th ed.; Wiley: New York, 1976.
(18) Fröhlich, H. *Adv. Phys.* **1954**, *3*, 325.
(19) Adachi, S. *J. Appl. Phys.* **1985**, *58*, R1.
(20) Kornilovitch, P. E. *Phys. Rev. B* **2006**, *73*, 094305.
(21) Shluger, A. L.; Stoneham, A. M. *J. Phys.: Condens. Matter* **1993**, *5*, 3049.
(22) Holstein, T. *Ann. Phys.* **2000**, *281*, 725.
(23) Austin, I. G.; Mott, N. F. *Adv. Phys.* **2001**, *50*, 757.
(24) Honig, J. M. *J. Res. Dev.* **1970**, *14*, 232.
(25) Stoneham, A. M.; Gavartin, J.; Shluger, A. L.; Kimmel, A. V.; Ramo, D. M.; Ronnow, H. M.; Aeppli, G.; Renner, C. *J. Phys.: Condens. Matter* 2007, *19*.
(26) Giannozzi, P.; de Gironcoli, S.; Pavone, P.; Baroni, S. *Phys. Rev. B* **1991**, *43*, 7231.
(27) Wagner, J.-M.; Bechstedt, F. *Phys. Rev. B* **2000**, *62*, 4526.
(28) Srivastava, G. P.; Tütüncü, H. M.; Günhan, N. *Phys. Rev. B* **2004**, *70*, 085206.
(29) Posternak, M.; Resta, R.; Baldereschi, A. *Phys. Rev. B* **1994**, *50*, 8911.
(30) Phillips, J. C. *Bonds and Bands in Semiconductors*; Academic: New York, 1973.
(31) Devreese, J. T. *Polarons in Ionic Crystals and Polar Semiconductors*; Springer: North−Holland, Amsterdam, 1972.
(32) Fu, Z.-W.; Qin, Q.-Z. *J. Phys. Chem. B* **2000**, *104*, 5505.
(33) Ottaviani, M.; Panero, S.; Morzilli, S.; Scrosati, B.; Lazzari, M. *Solid State Ionics* **1986**, *20*, 197.
(34) Kanamura, K.; Yuasa, K.; Takehara, Z. *J. Power Sources* **1987**, *20*, 127.
(35) Lindström, H.; Södergren, S.; Solbrand, A.; Rensmo, H.; Hjelm, J.; Hagfeldt, A.; Lindquist, S.-E. *J. Phys. Chem. B* **1997**, *101*, 7710.
(36) van de Krol, R.; Goossens, A.; Schoonman, J. *J. Phys. Chem. B* **1999**, *103*, 7151.
(37) Kavan, L.; Grätzel, M.; Gilbert, S. E.; Klemenz, C.; Scheel, H. J. *J. Am. Chem. Soc.* **1996**, *118*, 6716.
(38) Deskins, N. A.; Dupuis, M. *J. Phys. Chem. C* **2009**, *113*, 20998.
(39) Kerisit, S.; Rosso, K. M.; Yang, Z.; Liu, J. *J. Phys. Chem. C* **2009**, *113*, 346.
(40) Duzhko, V.; Timoshenko, V. Y.; Koch, F.; Dittrich, T. *Phys. Rev. B* **2001**, *64*, 075204.
(41) Hamdi, I.; Aouissi, M.; Qteish, A.; Meskini, N. *Phys. Rev. B* **2006**, *73*, 174114.
(42) Åberg, D.; Erhart, P.; Crowhurst, J.; Zaug, J. M.; Goncharov, A. F.; Sadigh, B. *Phys. Rev. B* **2010**, *82*, 104116.
(43) Beunetto, J.; Vanderbilt, D. *Phys. Rev. B* **1996**, *53*, 15417.